

Localization for Wireless Sensor and Actor Networks with Meandering Mobility

Mustafa İlhan Akbaş*, Melike Erol-Kantarci†, and Damla Turgut*

*Department of Electrical Engineering and Computer Science

University of Central Florida, Orlando FL

Email: {miakbas,turgut}@eecs.ucf.edu

†School of Information Technology and Engineering

University of Ottawa, Canada

Email: melike.erolkantarci@uottawa.ca

Abstract

Environmental monitoring applications for wireless sensor and actor networks rely on position estimation in order to process or evaluate the observed data. The absence of efficient positioning techniques for sensor nodes operating in harsh environments calls for novel approaches. While monitoring the Amazon river, unprecedented characteristics of the river and its surroundings challenge the node communications and drifting of the nodes makes it difficult to use the existing positioning methods. To address these challenges, we propose a multi-hop localization technique that takes advantage of sensor mobility with local information exchange. The collected information is used to enrich the environmental data with location information. The maximum hop distance for actor affiliation is also adapted according to network characteristics to improve energy consumption behavior. The motion of the sensor nodes follows the advection of the fluid parcels in the river, which is modeled as a combination of a central streamline with a meandering motion around the rough surface. This translates into a stretching topology with correlated motion for sensor nodes. Through extensive simulations, we show that the nodes can be efficiently positioned using the proposed approach, as our technique is compliant with the movement patterns of the sensor nodes in the realistic mobility model of the river.

I. INTRODUCTION

Wireless sensor and actor networks (WSANs) are geographically distributed systems with large number of tiny sensor nodes and a limited number of actors [1], [2]. Events in the environment are observed

by the sensor nodes, which have limited processing and communication capabilities. The more powerful actors collect information from the sensor nodes and react to the events with a physical action or by taking network related decisions. WSANs have a broad range of applications such as environmental monitoring, military surveillance, and intelligent transportation. Depending on the particular purpose of each application, the sensor nodes are equipped with proper sensor adapters with functions such as motion detection or temperature measurement for the accurate collection of any required data in their environment. In addition to the accurate observation methods, most applications also require location information to be associated with the collected data in order to deliver meaningful results [3]. Environmental monitoring is an application area in which the location of the gathered data is critical.

Amazon river is the subject of the environmental monitoring application considered in this work. Amazon is the largest river by waterflow in the world and it is also the second longest river with a difference of only 2.3%. The bulk of the river flows through a giant tropical rain forest, which restricts the access to the river. The massive volume with a drainage area of almost seven million square kilometers and the harsh basin conditions make the river difficult to monitor by human operators or by employing traditional methods such as sample collection. The utilization of a WSAN monitoring system would increase the quality in observation, investigation, and the response.

In this paper, we propose a WSAN based solution, in which the actors are positioned at specific accessible spots on the coastline of the river or on the small islands in the river, while the sensor nodes float on the water (see Fig. 1). Our previous work in this area [4] is extended with a realistic mobility model, an adaptation of the localization for this mobility model and an energy consumption analysis. As the sensor nodes move, they collect information about the environment and transmit the collected data to the actors. The collected data are analyzed at the actors to create time and location information and provide the characteristics of the river to the users. To utilize the monitoring results efficiently, it is critical in this environment to match the collected data with the position of a sensor node at any given time. In many scenarios, the collected data becomes unusable if not associated with the position and time. The paths of the nodes deliver additional information about the nodes and the environment such as current speed, direction, structure of the terrain or the obstacles in the river.

The main contribution of this work is the multi-hop locality preserving localization algorithm design, which enriches the collected environmental data with position information. For the creation of the hierarchical network structure of sensor nodes and actors, a network organization algorithm is also designed

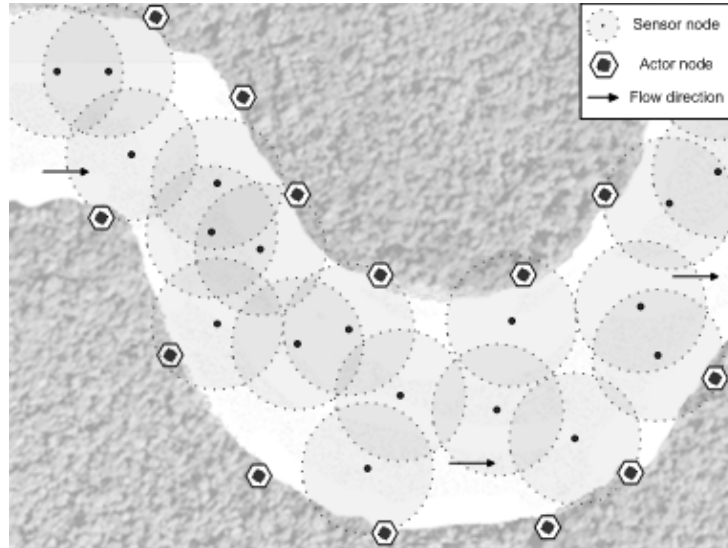


Fig. 1. The river monitoring scenario with floating sensor nodes and stationary actor nodes on the accessible spots.

and used along with lateration for localization. The organization in the network is dynamically adapted with the continuous change of the communication topology, turning mobility into an advantage for energy efficiency by eliminating the requirement for extra control messages. The accuracy of the event localization is improved by including path estimation in the algorithm. The affiliation area for each actor is also adapted according to the distances to other actors in terms of hop counts. This adaptation reduces the packets transmission and improves the energy consumption in the network.

The second contribution of this work includes the adaptation of a realistic mobility model [5] according to the requirements of the river scenario. Since the sensor nodes drift in the river with the force of the current and the use of a realistic current mobility model is critical to analyze the accuracy of the localization algorithm. Amazon river has a high water load and low slopes over the river basin, resulting in a meandering structure (see [6]). Therefore, a subsurface meandering current mobility model with random surface motion is incorporated into our algorithm taking the requirements of our scenario into consideration. To the best of our knowledge, this is the first example of using meandering current mobility model with random surface motion for the simulation of sensor and actor networks operating on the surface of a river.

Additionally, a basic directional mobility model is also created without considering the any specific characteristics of the river. This basic model is used to analyze the effects of the realistic mobility on the performance of the algorithm.

The remainder of this paper is organized as follows. Related work is summarized in Section II. The

localization algorithm is presented with the network layout and the mobility model in Section III. The validity and applicability of the proposed scheme is demonstrated with simulations in Section IV and we finally conclude in Section V.

II. RELATED WORK

Localization is defined as the process of estimating the positions of nodes in an environment and it has been attracting significant interest in wireless sensor networks (WSN) research domain as the multifunctional sensor nodes have been deployed in both indoor and outdoor environments [7]. The implementations of localization techniques in WSNs and WSANs have their particular constraints. For instance, WSANs are generally deployed in harsh environments and they have challenges related to these harsh environments such as accessibility, line-of-sight, and so on. The heterogeneous node structure of WSANs is yet another challenge and the solutions require a clear differentiation of the roles of different node types in the network.

The localization methods in the literature generally use *a priori* information about the network or the environment such as the positions of some specific nodes [8] or particular locations in the environment where the nodes can be located at [9]. Localization algorithms also make use of diverse scientific approaches such as graph theory [10], [11], multidimensional scaling [12], sequencing [13], distance vectors (DV) [14], computational geometry [15], particle and Kalman filters [9], [16], [17], Gauss-Markov parameter estimation [18], recursive systems [19], sub-area localization [20], range-free schemes [21], viable kernel-based algorithms [22] and distributed Bayesian algorithms [23].

The measurements of different types of sensors on the nodes can also be used by localization algorithms. Sensor nodes can gather various kinds of information when equipped with appropriate measurement technologies. The main types of sensor measurements used in localization methods are time of arrival (ToA) [24], time difference of arrival (TDoA) [25], angle of arrival (AoA) [26], received signal strength (RSS) [27], [28], and distance related measurements [29]. The measurement technique is normally selected according to the requirements of the environment and the scenario. Multiple techniques can also be utilized in a single approach. Wang et al. [30] propose using multiple techniques for an unsupervised indoor localization scheme, which identifies certain locations in an indoor environment with signatures on multiple sensing dimensions. Michaelides and Panayiotou [31] use RSS at the sensor nodes to report binary observations. The events are reported only when the measured signal strengths are above a threshold. These binary observations are used in an estimation algorithm to construct the likelihood matrix.

In the literature, there are also localization techniques that do not mainly rely on sensor measurements. For instance, Nagpal et al. [32] organizes a global coordinate system in the network by estimating the Euclidian distance of a hop. This estimation algorithm uses the number of communication hops of the sensor nodes and the position error is minimized with imperfect distance estimates. The important theoretical results given by Nagpal et al. are the critical minimum average neighborhood size for sufficient accuracy and the limit on the resolution of a coordinate system determined by local communication.

Some localization approaches are considered both centralized and distributed. Sheu et al. [33] use a distributed technique to estimate the location of the regular nodes by gathering the positions of location-aware nodes (anchor nodes) and the one-hop regular nodes whose locations are estimated from the anchor nodes. The paired measurement localization (PML) strategy of Rahman and Kleeman [34] is another distributed solution, which achieves accurate positioning by employing a theoretical minimum number of four anchor nodes.

We use a multi-hop localization method [4] and there are several examples of such approaches. The Ad-Hoc Positioning System (APS) by Niculescu and Nath [14] is a distributed hop-by-hop positioning algorithm. APS works as an extension of distance vector routing and GPS positioning. The positions of all nodes in the network are approximated by utilizing the information from a limited set of nodes, which have self localization capabilities.

Xiao et al. [35] construct a table for minimum hop length estimation by using the results of empirical studies. The threshold values in this table are used to filter out the unreliable anchors. Hence the sensor nodes determine their positions utilizing the data from reliable anchors. Yi et al. [36] propose a sequential Monte Carlo method based multi-hop localization technique for mobile networks with multiple sensor nodes and few anchor nodes. Wu et al. [37] define a new measure to propose a range-free localization method. The new metric is called regulated neighborhood distance (RND) and it is used to solve the ambiguity problem in cases when a node has the same distance estimation to all of its one-hop neighbors. RND relates the proximity of two neighboring nodes based on their neighbor partitions.

Our localization approach has unique characteristics, different from the previously discussed algorithms. We aim to determine the locations of the sensor nodes at the actors rather than the sensor nodes themselves, and the position information is not forwarded to the sensor nodes in contrast to previous work. Thus, our approach has the ability to resolve the location of the collected data or the events in an energy-efficient manner. The dynamic and continuous formation of the overlay network is another important part of our

approach. The weights and the affiliated actors of sensor nodes are assigned by an overlay network. For this purpose, the actor nodes are used as the clusterheads and the mobile sensor nodes are clustered by a multi-hop scheme with a set of locally acting rules as in SOFROP [38].

There are various clustering algorithms for mobile ad hoc networks in the literature with features specific to the application scenarios. The Weighted Clustering Algorithm (WCA) by Chatterjee et al. [39] is a distributed clustering algorithm for multi-hop packet radio networks and uses the ideal degree, transmission power, mobility, and battery power of mobile nodes for clustering decisions. Turgut et al. [40] have shown improvements on WCA's performance by using a genetic algorithmic technique. The problem formulation and the parameters are mapped to individual chromosomes to find the clusters for the optimum MAC layer operation. WCA is also extended by simulated annealing algorithm [41], which uses a random set of clusterheads and cluster members to determine the optimum solution defined by an objective function. Overlapping Clusters Algorithm (OCA) by Aydin et al. [42] uses battery and bandwidth capacity, transmission range, density, mobility, and buffer occupancy to determine the initial clusterheads. The states of these parameters are then continuously monitored to update the topology through reclustering when it is required. Hybrid Energy-Efficient Distributed (HEED) [43] clustering by Younis and Fahmy periodically selects clusterheads according to a hybrid of residual energy and another parameter chosen according to the requirements of the scenario.

High mobility of sensor nodes with the currents in the river is a distinct constraint of Amazon river scenario and it is considered as a challenge in most of the existing localization methods. The realistic modeling of the river and therefore the mobility of sensor nodes is an important part of our approach. We modeled the mobility as a correlated motion with random perturbations on the surface of the water. There have been studies on the formulation of the current mobility models. For subsurface ocean currents, Caruso et al. [5] proposed Meandering Current Mobility (MCM) model, extended later by addition of random surface motion by Erol et al. [44]. As an important difference compared to the ocean characteristics, the subsurface currents have faster speeds. On the other hand, the force of the winds and the shape of the terrain (rocks, depth/width variations) generate vortexes in a river, similar to oceans where the particles meander similar to the meanders in the MCM model.

III. LOCALIZATION

A. System model and mobility

We consider a wireless sensor and actor network N with the number of nodes $|N| = n$. N consists of a set of actor nodes A and a set of sensor nodes S . Our model also includes a sink node responsible for data aggregation and connection of the environmental monitoring network to a backbone network. The sensor nodes and actors are assumed to have maximum transmission ranges r_s and r_a , respectively, with circular transmission areas, where $r_s < r_a$ due to better computation and communication capabilities of the actors. Every node is able to communicate only with its current one-hop neighbors, forming a locality preserving communication system.

Sensor nodes in the application scenario are deployed without any positioning adaptors. Positioning devices such as GPS receivers are avoided to enable longer network lifetime with the limited resources of sensor nodes. Besides long life-time requirements, the thick forest structure of Amazon is also a disadvantage for satellite communication. Therefore obtaining location information by GPS is not a viable option in Amazon river monitoring scenario. In our system, sensor nodes do not keep position information and each sensor node directly communicates only with its immediate neighboring nodes. The neighboring nodes of a sensor node can be both actor and sensor nodes. The local information of a sensor node is forwarded to the actors via intermediate nodes. The actors acquire their positions either from an external source or the position information is encoded in the deployment phase.

Actors are positioned on the coastline or on the islands of the river such that each one has at least one actor in its transmission range. The selection of actor positions and the actor network affects the performance of the localization approach. However, the main focus of this work is localization; therefore, actor positioning is not analyzed in detail. Actors use their full transmission ranges only when communicating with other actors. The network among the actors serves as the layout network for the processing of the collected data. This layout network is formed by selectively flooding the network formation packet among actor nodes. Each actor sets the neighboring actor in which the first network formation packet is received from, as the destination for the collected monitoring data. Therefore the neighboring node of an actor is another actor in this layout network. Then, an actor can receive additional network formation packets. The actors, from which these packets are received from, are saved in a list to be used in cases such as a change in the communication backbone.

When communicating with sensor nodes, the actor nodes use the same transmission range as the sensor

TABLE I
MOBILITY PARAMETERS

| | |
|------------|-----------------------------|
| $B(t)$ | Meander amplitude |
| ϵ | Degree of chaotic advection |
| ζ | Direction of flow |
| ξ | Width of the jet |
| h | Wave number |
| L | Wavelength |
| c_x | Phase speed |

nodes in order to have a bidirectional connection and save energy. The actor nodes continuously transmit packets encoded with their IDs and exchange packets with the sensor nodes in their transmission ranges. Sensor nodes retransmit the packets from actors to their direct neighbors. Each sensor node obtains its current neighbor information as it receives these retransmitted packets. Therefore the neighbor a sensor node can be both an actor or a sensor node.

The monitoring network aims to collect data from the unreachable parts of a river by allowing sensor nodes to drift with the force of the river currents. This uncontrolled motion of the sensor nodes follow the trajectories of the fluid parcels, making the mobility pattern more complex than the traditional random way point mobility or the group mobility models. The behavior of the network in the natural conditions of the river cannot be modeled with an assumption of a simple mobility pattern for the sensor nodes. Therefore, the movements of the sensor nodes must be modeled according to the properties of the river currents.

The motion of the subsurface currents in a river has several characteristic features. The advection in a river is affected from the variations in water depth, channel geometry, and the surface conditions. In a relatively short section of the river, the terrain can be assumed to force a higher volume of flow in the center line. Therefore, the velocity of the particles or the sensor nodes at the central stream will be higher than the ones closer to the boundaries. Furthermore, roughness of the surface may lead to eddies where the sensor nodes will be captured for a while and then possibly released to join the remaining part of the network. To model these properties, we adopt the motion of the subsurface currents, initially employed in [5], [44]. Table I summarizes the parameters used in subsurface current mobility model.

The channel geometry of the river will mandate time varying meander amplitude which is denoted as follows:

$$B(t) = B_0 + \epsilon \cos(\omega t + \theta) \quad (1)$$

Here, ϵ determines the degree of chaotic advection, where for relatively large ϵ , the particles are able to cross the jet in north to south direction or vice versa [45]. To model the currents in a river, we select ϵ such that the sensor nodes are allowed to mix with the jet stream. The direction of flow is denoted by ζ and it is defined as follows:

$$\zeta = \tan^{-1}\{B(t)h \cos[h(x - c_x t)]\} \quad (2)$$

Then, the motion of the sensor nodes can be defined with the following standard stream function [46]:

$$\Gamma(x, y, t) = \Gamma_0 \left\{ 1 - \tanh \left[\frac{y - \eta}{\xi / \cos(\zeta)} \right] \right\} \quad (3)$$

where ξ is the width of the jet and $2\Gamma_0$ is the total eastward transport.

The time-varying central streamline is defined by η and it is given by the following equation:

$$\eta = B(t) \sin[h(x - c_x t)] \quad (4)$$

where h is the wave number defined in relation to the wavelength L , as $h = 2\pi/L$, and c_x is the phase speed of the sinusoidal meander [47].

Eq. (3) represents the velocity field for an isopycnal surface where it is relevant to assume that sensor nodes can easily adapt to pressure changes since they already carry pressure sensor nodes as part of their monitoring task. To obtain the non-dimensional eastward moving frame, we substitute $x' = x - c_x t$ in ξ and in Eq. (4). Thus, Eq. (3) takes the following form:

$$\Gamma(x', y') = \Gamma_0 \left\{ 1 - \tanh \left[\frac{y' - \eta'}{\xi / \cos(\zeta')} \right] \right\} + c_x y' \quad (5)$$

From Eq. (5), the velocity of a sensor node is computed by a simple derivation as follows:

$$u = \frac{dx}{dt} = -\frac{\partial \Gamma}{\partial y}, v = \frac{dy}{dt} = \frac{\partial \Gamma}{\partial x}. \quad (6)$$

In addition to the subsurface current mobility model, a basic directional mobility model is used to

investigate the performance of the localization algorithm in different mobility conditions. In this second mobility model, each sensor node floats in the watercourse from a predetermined origin on one side of the river to a randomly chosen destination on the other side on a linear path.

B. Location estimation

The main goal of our location estimation approach is to enhance the environmental monitoring information collected from the river and create a detailed set of data with location and time information for a complete analysis of the river characteristics. Therefore, in contrast to most of the existing localization algorithms, the sensor nodes are not informed about their positions. This way, no computation is specifically required by the localization algorithm at the sensor nodes.

The mechanism for actor affiliation utilizes the “weight” values of the nodes. Each actor is assigned to a *weight* k , which is initialized with the same value for all actors in the beginning of system deployment. The initial k value is based on the characteristics of the network such as the communication ranges of the nodes or the physical constraints of the environment. Sensor nodes store *weight* values for the actors they are affiliated with. There is no initial configuration on the sensor nodes to affiliate them with the actors. The only data available for a sensor node s as it floats in the river are the direct neighbors $Neigh(s)$ and their corresponding *weights*, $w(Neigh(s_i))$.

The list of the *weights* for the actors, which a sensor is affiliated with, is stored in a “weight table”. The sensor nodes initially take random *weight* values between 0 and $k - 1$. The *weight* value of each affiliation is updated according to “hop distance”, h , of the node to the actor in which it gets updates from. Therefore the *weight* $w_a(v)$ of a sensor node v for an actor a is as follows:

$$w_a(v) = k_a - h_a(v)$$

The actors exchange packets with the sensor nodes in their transmission ranges. Each actor encodes the transmitted packets with its ID and *weight* k , denoting that the packet is originated at an actor. Each sensor node updates the *weight* values in its record via local updates. Thus the information about each actor is distributed and updated at the affiliation area of that actor.

A sensor node is capable of being affiliated with multiple actors and keeps the maximum *weight* for each actor it receives the packets from, as depicted in Fig. 2. The structure of the network is created as the sensor node continuously adapts its *weight* according to its local neighborhood. For each of its affiliated

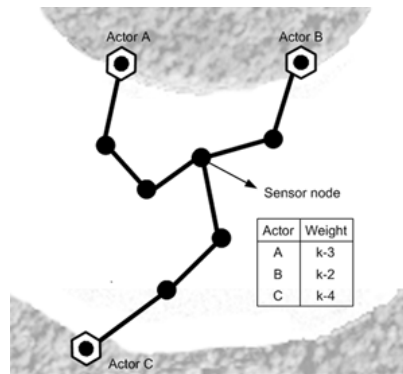


Fig. 2. Sensor node affiliated with multiple actors.

actor nodes, a sensor node's *weight* depends on the highest neighbor *weight*, M for that actor. The sensor node is assigned with the *weight* value of $M - 1$ unless it already has the same *weight* value. Hereby a hierarchical structure is dynamically formed and updated by creating an ordered tree structure. Therefore a sensor retransmits a packet received from an actor only if the *weight* value is less than the sensor node's *weight* for that actor. Otherwise the sensor node drops the packet to avoid unnecessary traffic and energy consumption in the network.

If the neighbors of a sensor node affiliated with an actor, have zero *weights*, then that sensor node cannot affiliate with that actor and it is out of the coverage area. When a sensor node loses its connection with all the actors and doesn't receive any *weight* updates, it operates only in "listening" mode. Listening nodes are physically able to exchange packets with neighbors having *weight* zero; however, there is no communication among these nodes. Algorithm 1 describes the state transitions for a node depending on its actor affiliation.

Algorithm 1 Sensor node weight assignment

- 1: $w_a(v)$: The *weight* of node v for actor a
 - 2: $\max(w(Neigh(v_a)))$: M
 - 3: **if** v is not affiliated with an actor node **then**
 - 4: $w_a(v) = 0$
 - 5: **else if** $M = k$ **then**
 - 6: $w_a(v) = k - 1$
 - 7: **else if** $M \neq k$ & $M > w_a(v)$ **then**
 - 8: $w_a(v) = M - 1$
 - 9: **else if** $M < w_a(v)$ **then**
 - 10: $w_a(v) = w_a(v) - 1$
 - 11: **else if** $Neigh(v_a) = \emptyset$ **then**
 - 12: $w_a(v) = 0$
 - 13: **end if**
-

When floating in the river, some sensor node groups can lose connection to the actors and particular

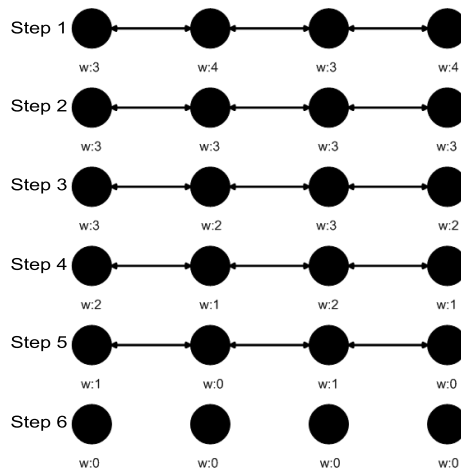


Fig. 3. Weight adaptation for a group of sensor nodes.

nodes in the group can have *weights* higher than all of their neighbors without having any affiliations to the actors. According to the hierarchical clustering *weight*, these nodes attract surrounding sensor nodes with lower *weights*, which would cause unnecessary data traffic since nodes with lower *weights* would transmit monitoring data towards the nodes with higher *weights*. This is prevented in the algorithm by successively reducing the *weight* of a node when it has the highest *weight* among its neighbors. The *weight* adaptation continues until connecting to an existing actor or until the *weight* of the node becomes the minimum value for the network.

Fig. 3 shows an example of a group of listening sensor nodes and their *weight* (depicted as w in Fig. 3) adaptation. All the nodes in this example are assumed to preserve their hop-distance to their neighbors during the specified period of time and k value for the network is set to five. The situation in Fig. 3 can be considered as the time when this group of four nodes just lost connection to an actor. Therefore none of the nodes is affiliated with an actor. As can be seen in Fig. 3 the weight adaptation terminates at sixth step when all the nodes have $w = 0$. In a realistic river environment, the neighbors of the nodes change continuously with mobility.

The sensor nodes update their position related data locally as the network topology changes due to node mobility. The sensor nodes affiliated with an actor form the “affiliation area” of that actor. Therefore, the selection of the k value for the actors is critical for the energy consumption in the network. In our algorithm, actor nodes adapt their k values according to their observations.

Each actor initializes k with a predetermined value (depending on the size of the network area). If the k value of an actor changes, the actor announces this change to the other actors. As the sensor nodes float into the reception range of actor nodes, they start to form and update their *weight* tables as shown

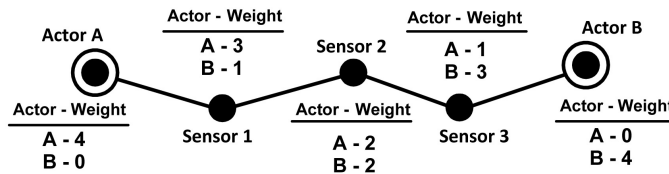


Fig. 4. The *weight* tables of sensor nodes affiliated with two actors.

in Fig. 4. Actors also keep *weight* values for the other actors with the same method. Then, each actor computes k_u value for all of its neighboring actors as follows:

$$k_u = \frac{k_n - w_n}{2}$$

where k_n is the k value stored for the neighbor actor n and w_n is the *weight* value of the neighboring actor n . Hence, k_u value for each neighbor actor is calculated according to the minimum number of hops between two actors. The k_u values are updated continuously such that the minimum is stored in the records for each neighbor actor.

The actor's k value is updated with the maximum of the k_u values. Actors have their location information, so the distance (d) between two actors, $i = 1, 2$, is calculated simply by using the Pythagoras theorem:

$$d^2 = (x_1 - x_2)^2 + (y_1 - y_2)^2$$

The adaptation of k arranges the size of the affiliation area for each actor according to the distances to other actors.

A decrease in the number of packets transmitted in turn reduces the total energy consumption in the network. Each sensor node communicates only with its 1-hop neighbors and the energy consumed to convey the collected information to an actor depends on the hop count of the node.

The packets originated from a sensor node v are transmitted to an actor a over a path of $h_a(v)$ hops. Hence the maximum number of transmissions in the actor area of a with n sensor nodes would be defined as $\sum_{i=1}^n h_a(v_i)$ when each sensor node transmits a packet. Then the improvement of the consumed energy in an actor area can be defined as follows:

$$E_i = \sum_{i=1}^n h_i - \sum_{j=k_a}^n h_j$$

The number of nodes in an actor area (n) decreases as the k value is adapted according to the neighbor actors. If the distance to the furthest neighbor actor is d_a , the adapted k value (k_a) can be assumed to be $\frac{d_a}{2}$. Then the number of sensor nodes affiliated with an actor can be approximated in proportion to the change in the actor area, as $n \frac{d_a^2}{4r_s^2k^2}$ improvement of the consumed energy in an actor area is denoted as follows:

$$E_i = h_{av} \left(n - n \frac{d_a^2}{4r_s^2k^2} \right)$$

where h_{av} is the average hop value of the sensor nodes, which are not affiliated with the actor a with the adaptation of k . In a uniform distribution of the sensor nodes, h_{av} is greater than $\frac{1}{2} \left(\frac{d}{2r_s} + k \right)$. Hence the improvement in energy can be approximated as follows:

$$\begin{aligned} E_i &= \frac{1}{2} \left(\frac{d_a}{2r_s} + k \right) \left(n - n \frac{d_a^2}{4r_s^2k^2} \right) \\ &= \frac{nd_a}{4r_s} \left(1 - \left(\frac{d_a}{2r_s k} \right)^2 - \frac{d_a}{r_s k} \right) + \frac{nk}{2} \end{aligned} \tag{7}$$

The adaptation of k is also important for the hop-distance estimation since the values calculated with this method are used when estimating the locations of the sensor nodes. The adaptation of k forces sensor nodes to be affiliated only with actors in close proximity which reduces the negative impact of the dynamically changing topology.

An actor keeps different k values for all the other actors that they store *weight* values for. These values are used in the calculation of “1-hop distance”. The average 1-hop-distance value is estimated as $\frac{d}{2k_u}$ and this calculated value is used for localization purposes. The sensor nodes dynamically store and update their *weights* as they float in the network. Actors collect weight information when the data packets are transmitted to the actors. Sensor nodes piggyback their *weight* tables to the data packets and these tables are used to estimate the distances of the nodes to the actors. The estimated distance of a sensor node to an actor A is calculated as follows:

$$d_A = (k_A - w_A) * h_A$$

where d_A is the estimated distance to the actor A , w_A is the *weight* of the sensor node for the actor A and h_A is the average 1-hop distance of actor A .

The distance estimation is based on the number of hops needed to reach from the sensor nodes to the actor nodes. Therefore it's similar to the distance vector (DV) based approach of Niculescu and Nath's model [14]. However, their model is designed for static networks and additionally, in most of the DV-based solutions, sensor nodes need to assign a fixed memory to save the locations of all the landmarks, hop-counts to these landmarks and average hop-distance values. In our approach, a sensor node stores only the *weight* values for a small set of actor nodes. All the other computation and memory requirements of the algorithm are handled by the actors and the sink, which is a better-fit for WSN structure in terms of the usage of memory, computational resources and energy. Hereby, the information flooding, which is common and intense in DV-based solutions, is also minimized.

When a sensor node's *weight* values are collected for three actors, its distances to these actors are estimated according to the "1-hop distance" value and the *weights*. The estimated distance of a sensor node is calculated for each of the actors it's affiliated with and then these values are plugged into the iteration operation for the estimation of the sensor nodes position. When a sensor node is affiliated with multiple actor nodes, its position estimation can be represented with a system of equations, written in matrix form as follows:

$$\begin{bmatrix} 2(x_n - x_1) & 2(y_n - y_1) \\ \vdots & \vdots \\ 2(x_n - x_{n-1}) & 2(y_n - y_{n-1}) \end{bmatrix} \begin{bmatrix} x_s \\ y_s \end{bmatrix} = \begin{bmatrix} (d_1^2 - d_n^2) - (x_1^2 - x_n^2) - (y_1^2 - y_n^2) \\ \vdots \\ (d_{n-1}^2 - d_n^2) - (x_{n-1}^2 - x_n^2) - (y_{n-1}^2 - y_n^2) \end{bmatrix}$$

where (x_i, y_i) , $(i = 1, \dots, n)$, are the positions of the n actors and d_i , $(i = 1, \dots, n)$, are the estimated distance values.

The solution pair of this system, (x_s, y_s) , minimizes $\|\mathbf{Ax} - \mathbf{B}\|_2$ value. This pair also minimizes the mean square error, where $0.5\mathbf{A}$ is the left hand side matrix, \mathbf{B} is the right hand side matrix and \mathbf{x} is the vector for (x_s, y_s) pair. Since $\|\cdot\|_2$ is minimized, the system is solved with minimum average error for all positions of the actors that the sensor is affiliated with.

For any vector \mathbf{v} , $\|\mathbf{v}\|_2^2$ is equal to $\mathbf{v}^T \mathbf{v}$, which can be used to find a solution for \mathbf{x} . Therefore, if the same expression is written for $\|\mathbf{Ax} - \mathbf{B}\|$, an equation for \mathbf{x} can be found:

$$\|\mathbf{Ax} - \mathbf{B}\|_2^2 = \mathbf{x}^T \mathbf{A}^T \mathbf{Ax} - 2\mathbf{x}^T \mathbf{A}^T \mathbf{B} + \mathbf{B}^T \mathbf{B}$$

This expression is minimized when the mean square error is minimized. Therefore, the gradient of the expression must be set to zero considering it as a function of \mathbf{x} :

$$2\mathbf{A}^T \mathbf{Ax} - 2\mathbf{A}^T \mathbf{B} = 0 \Leftrightarrow \mathbf{A}^T \mathbf{Ax} = \mathbf{A}^T \mathbf{B}$$

This is the normal equation for the linear least squares problem and it has a unique solution. We use the Cholesky factorization to solve this equation and to get the estimations for x and y coordinates of the sensor nodes. Accordingly, the resulting matrix is given by:

$$\mathbf{x} = (\mathbf{AA}^T)^{-1} \mathbf{A}^T \mathbf{B}$$

The estimations for the coordinates of the sensor nodes are calculated by this method for each time instance and recorded. Since our goal is not an online location-awareness for the sensor nodes, the paths followed by the nodes are estimated after these points are calculated. Essentially, the paths are estimated using the interpolation of these coordinates. Hence, the effect of the errors in the individual estimates to the paths of the sensor node is minimized.

IV. SIMULATION STUDY

In this section, we evaluate our approach by measuring how the errors in the estimated locations vary with the characteristics of the localization algorithm and the mobility model in use. The simulation study is conducted in OPNET Modeler [48]. Table II summarizes the parameters used in our simulation study. The settings are chosen according to the requirements of Amazon scenario. The actor nodes are stationary, deployed in an area uniformly at random with the constraint that they are able to form a connected graph. Sensor nodes are mobile and they are flowing in the watercourse. The basic directional mobility model and the meandering mobility model are used in different experiments to define the movement of the sensor nodes. The communication links among the sensor nodes are assumed to be prone to failures due to shadowing and multipath caused by the river environment.

TABLE II
SIMULATION PARAMETERS

| | |
|--------------------------------------|------------|
| Number of sensor nodes | 100 |
| Number of actor nodes | 25 |
| k value | 1-5 |
| Terrain size | 200×1400 m |
| Sensor node transmission range | 40 m |
| Average jet speed | 1-7 m/s |
| Degree of chaotic advection | 0.3 |
| Frequency of time dependent meanders | 0.4 |
| Simulation time | 3600 s |

A. Clustering

Clusters formed as the sensor nodes move in the network play an important role for localization accuracy. The number of actors, which a sensor node can be affiliated to, increases with increasing k . These affiliations and the parameter k are included in the hop distance estimations. Therefore, the localization accuracy is affected by their values.

In the first set of experiments, the parameter k is set to a small value ($k = 2$) to observe the performance of the algorithm in a low clustering scenario. This value minimizes the influence of clustering by limiting the maximum number of hops between a sensor node and its affiliated actor node. Therefore, in this case, only the sensor nodes, which can reach the actor through one or two hops are allowed for affiliation. The experiments are conducted for both the meandering and the basic directional mobility models. The error distribution of localization with the basic directional mobility is illustrated in Fig. 5. The error distribution when using meandering mobility model with average jet speed of 1.5 m/s is shown in Fig. 6.

In the second set of the experiments, the value of the parameter k is increased to five. The goal of these experiments is to observe the influence of clustering in the location estimation by comparing the results of the first set to the second set of experiments. The location estimation error distributions are illustrated in Fig. 7 and Fig. 8 for basic directional and meandering mobility models, respectively.

The localization error has a normal distribution for both values of the parameter k . When $k = 2$, the range of the error is between -25 and 25 meters for both mobility models. The estimation errors are equal to or below 15 meters for $\sim 93\%$ of the results in basic directional mobility and $\sim 97\%$ of the results in meandering mobility model. When k is increased to five, the range of the error results is more than the results observed in the first experiment. Since the number of affiliations increases as k increases, we also observe that the number of estimated points is higher when k is five. When the meandering mobility

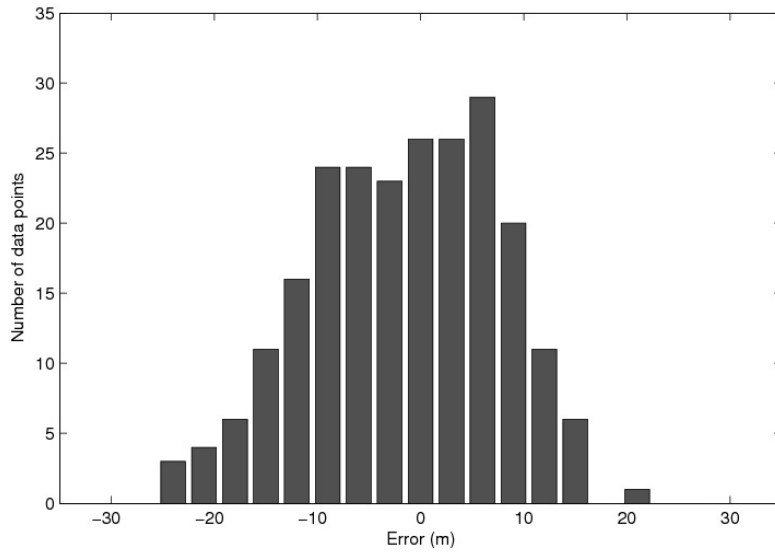


Fig. 5. The error distribution of the estimation results with basic directional mobility and $k = 2$.

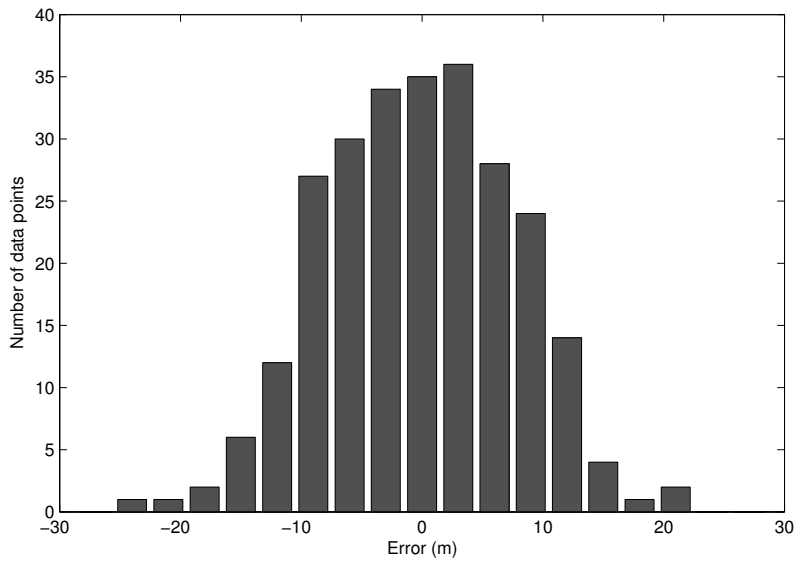


Fig. 6. The error distribution of the estimation results with meandering mobility and $k = 2$, average jet speed = 1.5 m/s.

model is used, the error is below 40 meters for 73% of the results. These simulation results show that as the length of communication paths are allowed to become larger, more positions can be estimated with a cost on the accuracy. When the number of estimated positions doesn't satisfy the requirements of an application scenario, a larger k value may be preferred for the next set of observations. Therefore, the selection of the maximum hop number depends on the requirements of the network under consideration and the scenario.

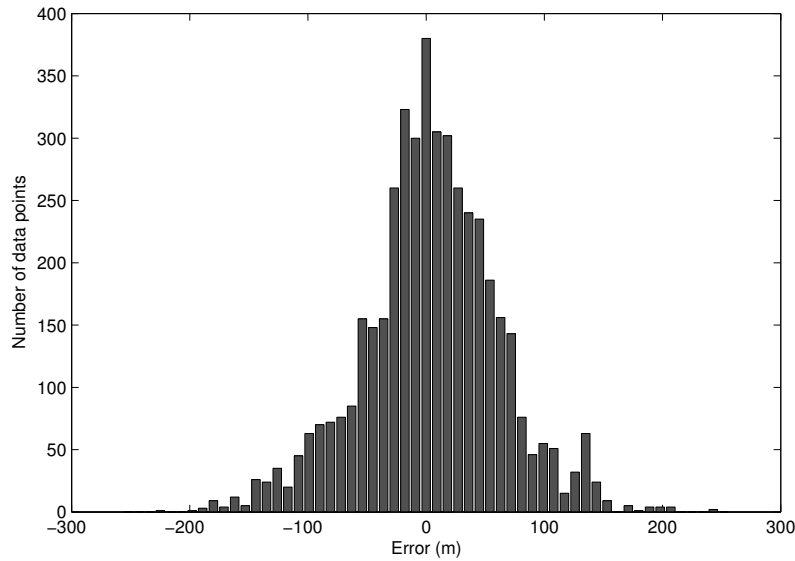


Fig. 7. The error distribution of the estimation results with basic directional mobility and $k = 5$.

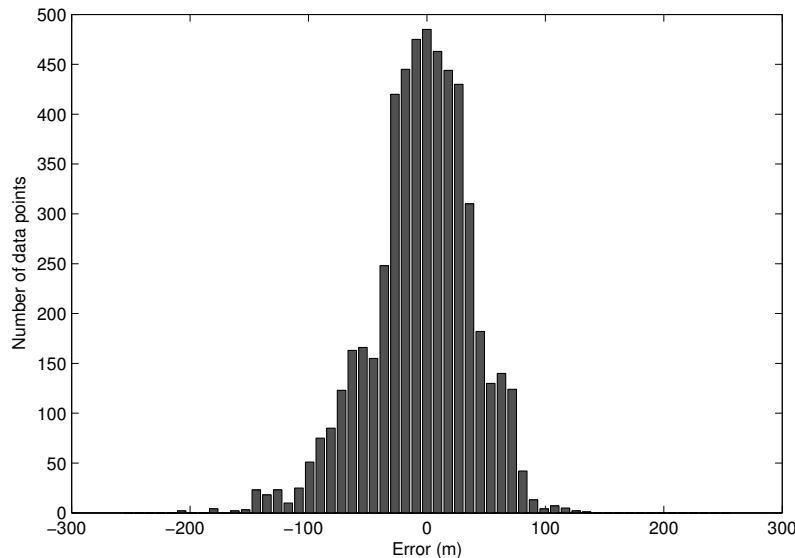


Fig. 8. The error distribution of the estimation results with meandering mobility and $k = 5$, average jet speed = 1.5 m/s.

B. Mobility model

In this experiment set, the impact of the mobility model on the performance of the localization algorithm is evaluated. The movement of sensor nodes is modeled with meandering and the basic mobility models, where the parameter k is set to three and the average jet speed used is 1.5 m/s. The error distribution results are illustrated in Fig. 9 and Fig. 10 for basic directional and meandering mobility models, respectively.

Using the results of this experiment set and the previous one, from Fig. 5 to Fig. 10, we observe that the error has a normal distribution for both models, while the number of data points is larger for meandering mobility model. The difference in the number of data points is higher for low error values in favor of the

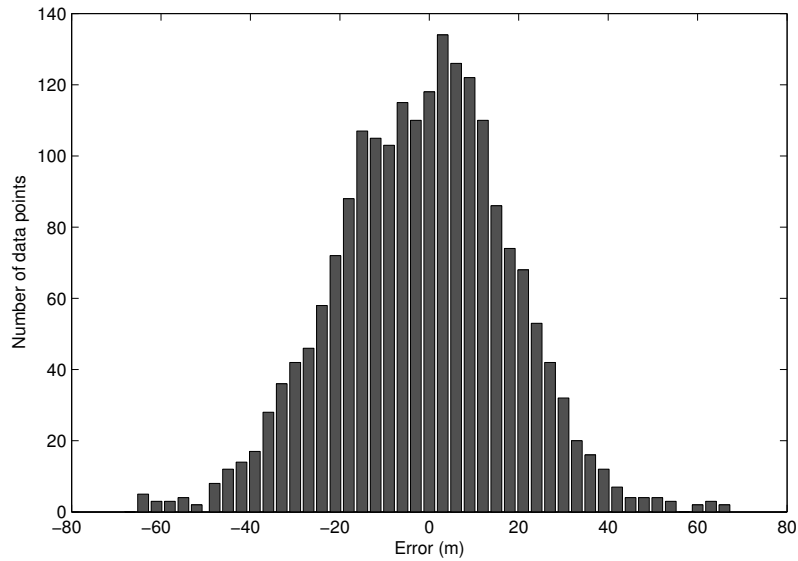


Fig. 9. The error distribution of the estimation results with basic directional mobility and $k = 3$.

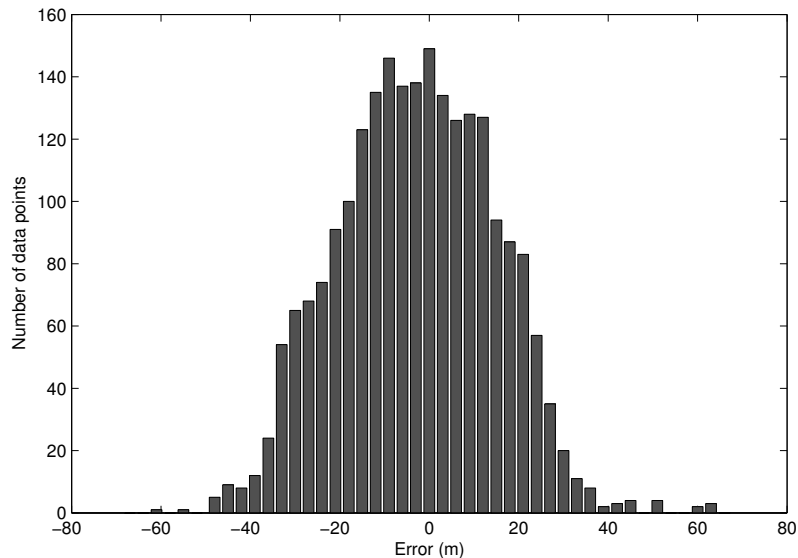


Fig. 10. The error distribution of the estimation results with meandering mobility and $k = 3$.

experiments with meandering mobility model, which shows that the accuracy of the algorithm is better with meandering mobility model.

The location estimation is also demonstrated for particular sensor nodes in the experiments to observe the accuracy of the algorithm. Fig. 11 and Fig. 12 show the exact trajectory of one of the sensor nodes on the x coordinate and the estimations of our algorithm for both mobility models. Fig. 13 and Fig. 21 show the results of the experiment for y coordinate.

As it was observed with the error distribution results, the accuracy of the estimation results is higher with meandering mobility model. This is because of a stretching topology with correlated motion where

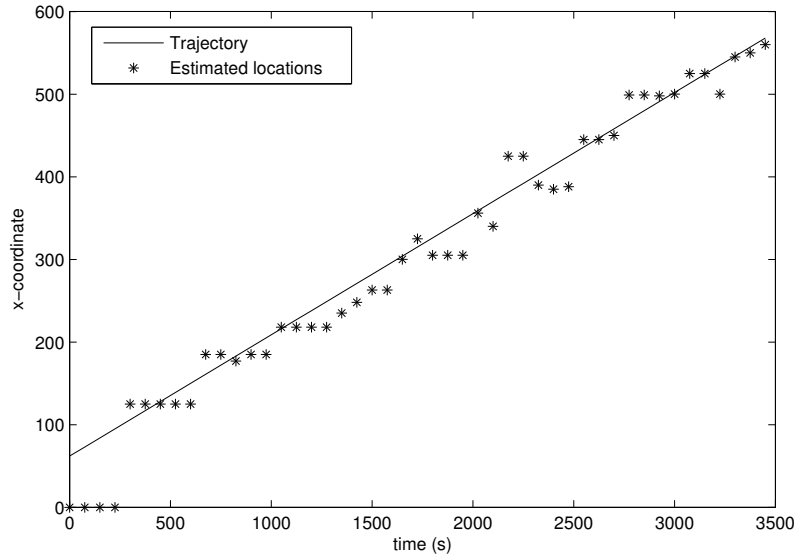


Fig. 11. Estimated x-coordinates and the real trajectory of a sensor node with basic directional mobility.

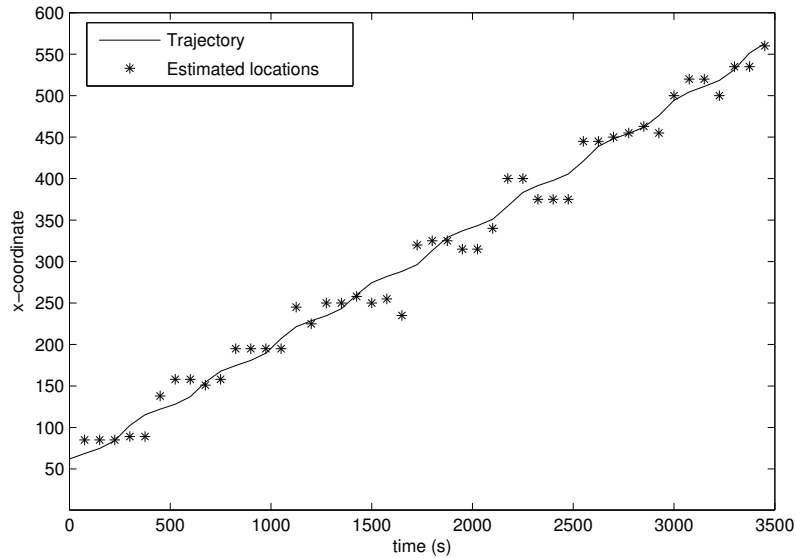


Fig. 12. Estimated x-coordinates and the real trajectory of a sensor node with meandering mobility.

some sensor nodes float behind others supplying reach for more actors when compared to random floating of the nodes in basic directional mobility. The localization algorithm gives better results when the sensor nodes move with meandering mobility. This is an advantage of the localization algorithm and denotes that the algorithm would have better performance in a real life scenario compared to a random mobility simulation due to realistic characteristics of the meandering mobility model.

The cost of our localization approach in terms of energy consumption is demonstrated in Fig. 15 with 95% confidence interval for different values of k . The energy consumption is observed for basic directional mobility model (BDM) and for meandering mobility model with (MMk) and without (MM) k

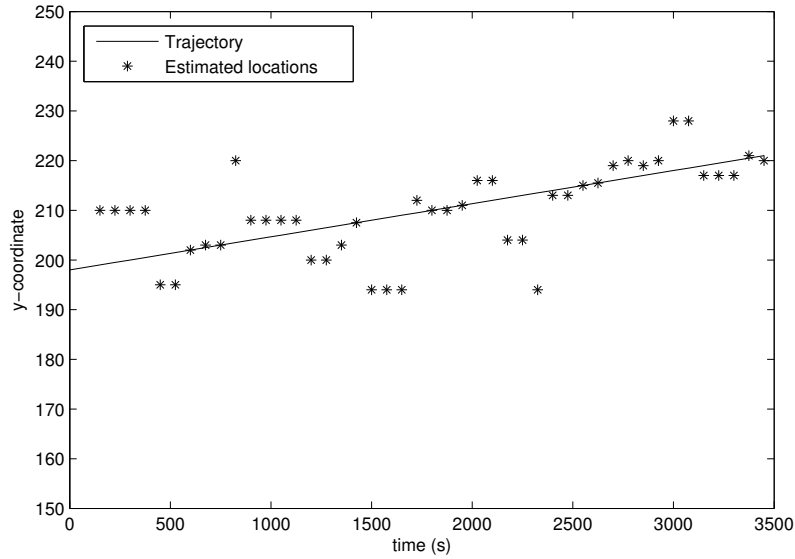


Fig. 13. Estimated y-coordinates and the real trajectory of a sensor node with basic directional mobility.

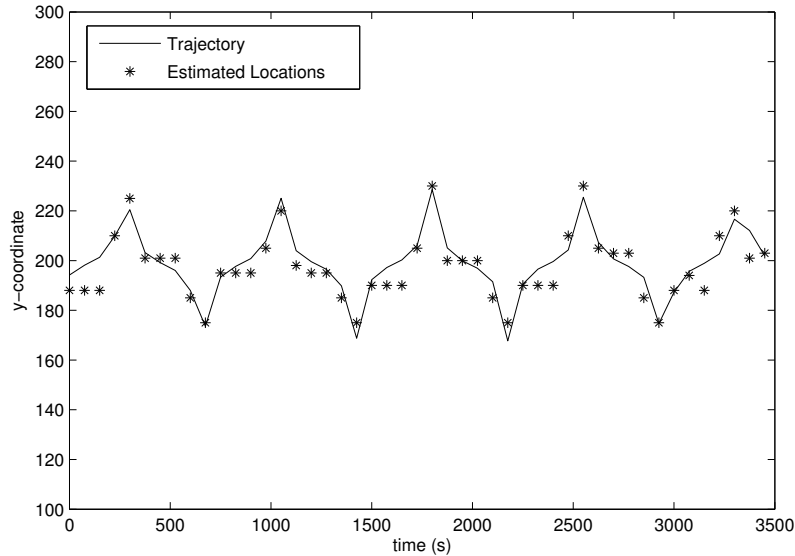


Fig. 14. Estimated y-coordinates and the real trajectory of a sensor node with meandering mobility.

adaptation. The energy consumption parameters of this simulation set are chosen from the multi-sensor system, which was deployed in the River Lee Co. Ireland [49]. Similar to our application scenario, this multi-sensor system is used to monitor water quality parameters such as pH, temperature or dissolved oxygen. According to the power consumption analysis of Regan et al. [49], the power consumption of a node in the simulation is 96.2 mW when the transceiver is active and 0.054 mW when the transceiver is not active.

One of the important results denoted in Fig. 15 is the effect of k in the energy consumption. The energy consumption increases with the increasing values of k . As shown in the results of error distribution exper-

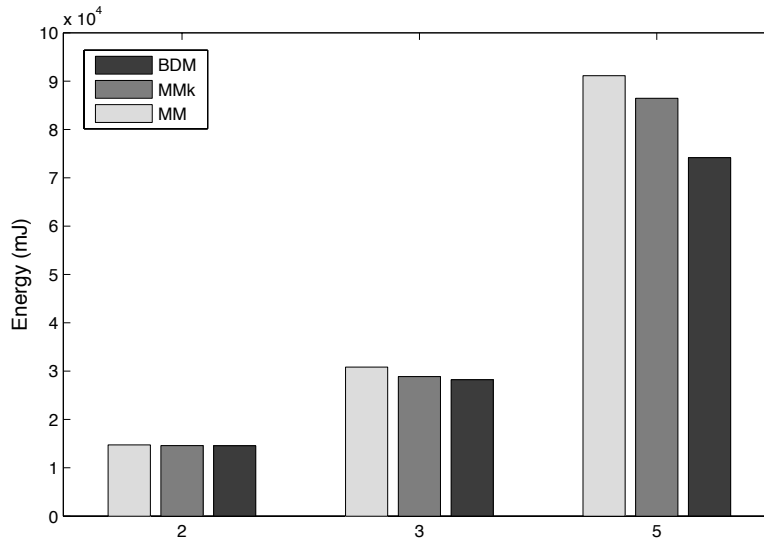


Fig. 15. Energy consumption for basic directional mobility, meandering mobility and meandering mobility with different k values.

iments, the collected data also increase with larger k values. Therefore, the number of data receptions and transmissions is larger for larger k values with the cost of an increase in energy consumption. Additionally, the energy consumption is higher for meandering mobility model and the difference accumulates as the value of k increases. Hence the higher clustered structure created by the meandering mobility model results in more data transmission and more energy consumption. The improvement in energy consumption by the adaptation of k is also observed in Fig. 15 and this effect becomes more apparent as k increases.

C. Meandering mobility

In the meandering mobility model, the average jet speed is an important factor to define the characteristics of the meandering behavior of the river current. For a comprehensive evaluation of the proposed localization approach, the average jet speed parameter of the meandering mobility model is varied in the next set of simulations.

Fig. 16 shows the paths for all sensor nodes in two examples from each of the simulation sets with average jet speed values varying from one to seven meters per second. Fig. 16 (a) and Fig. 16 (b) show the paths of nodes with the average jet speed of one meter per second. When the average jet speed is increased to three meters per second as presented in Fig. 16 (c) and Fig. 16 (d), the effect of this increase can be observed particularly in the meander amplitude. The jet speed is further increased to five meters per second in Fig. 16 (e) and Fig. 16 (f) and seven meters per second in Fig. 16 (g) and Fig. 16 (h). The variance in the y -coordinates of the sensor node positions decreases as the jet speed is increased.

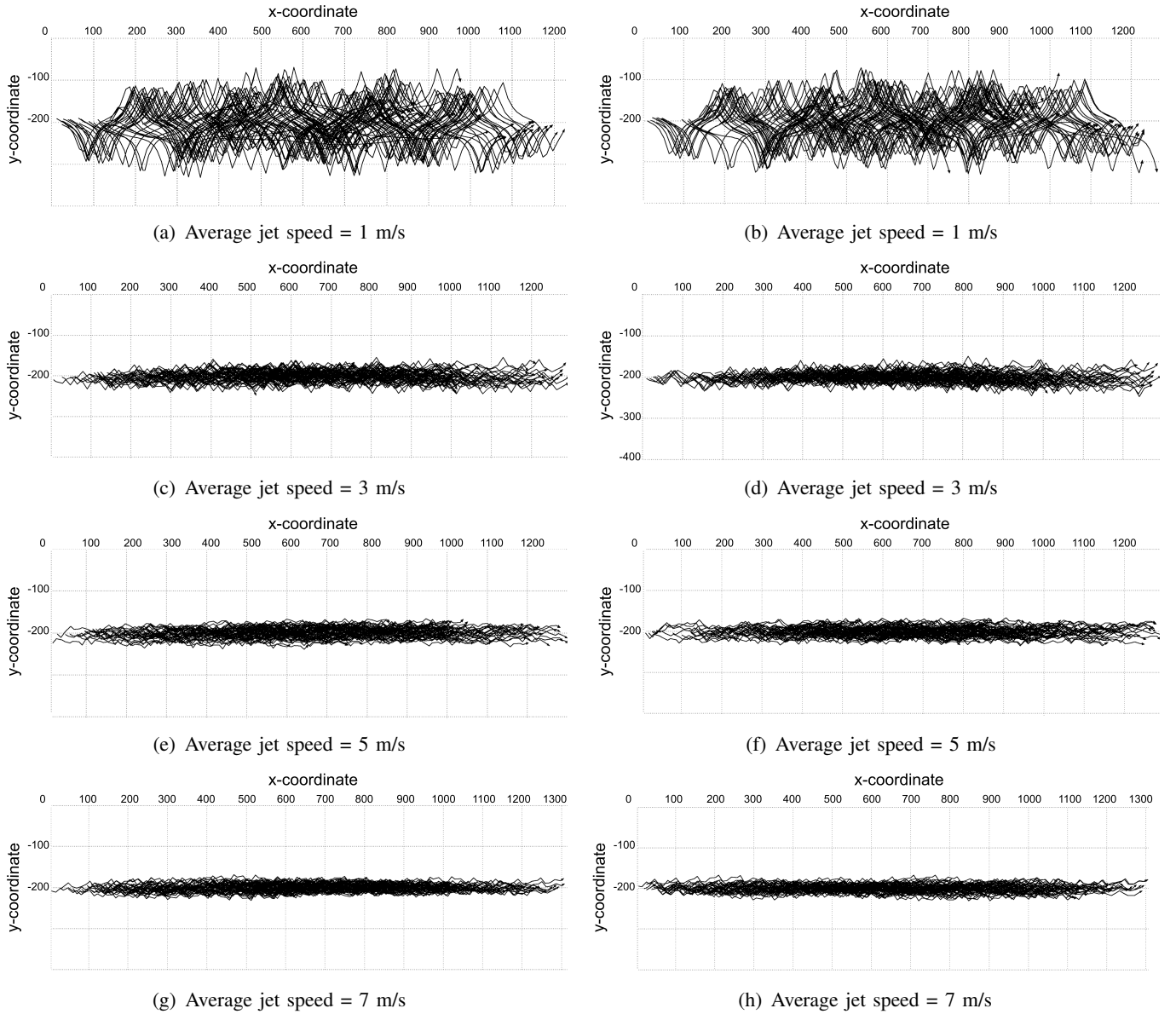


Fig. 16. Examples for the paths of 100 nodes with varying average jet speed values.

This characteristic of the mobility model can be used to adjust the values of the localization algorithm parameters for the specific requirements of different application scenarios.

Figs. 17-20 show the error distribution results of the location estimation for meandering mobility with the average jet speed values 1m/s, 3m/s, 5m/s and 7m/s, respectively.

The localization errors collected for the experiments with different average jet speed values have results close to each other. However the results also show that the accuracy of the position estimation increases for these four values with the increasing jet speed. The number of data points collected also increases as the meander amplitude decreases. This result can be explained with the additional stretching in the topology when the meandering jet amplitude decreases.

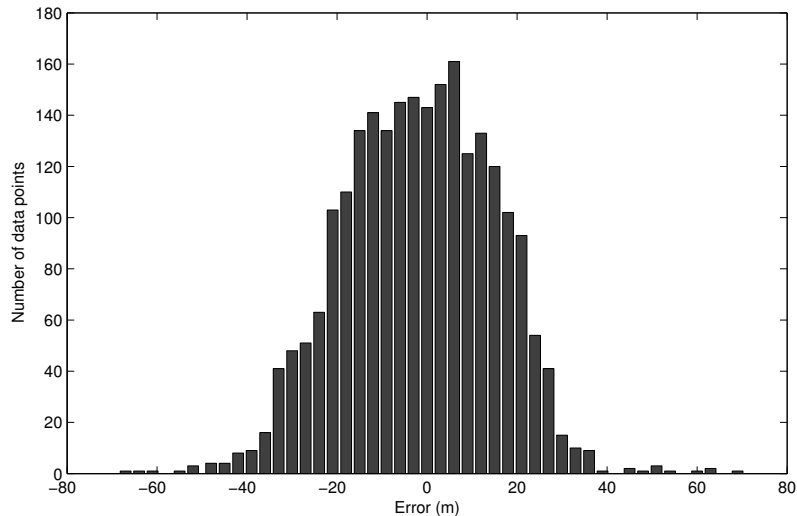


Fig. 17. The error distribution of the estimation results with average jet speed of 1 m/s and $k = 3$.

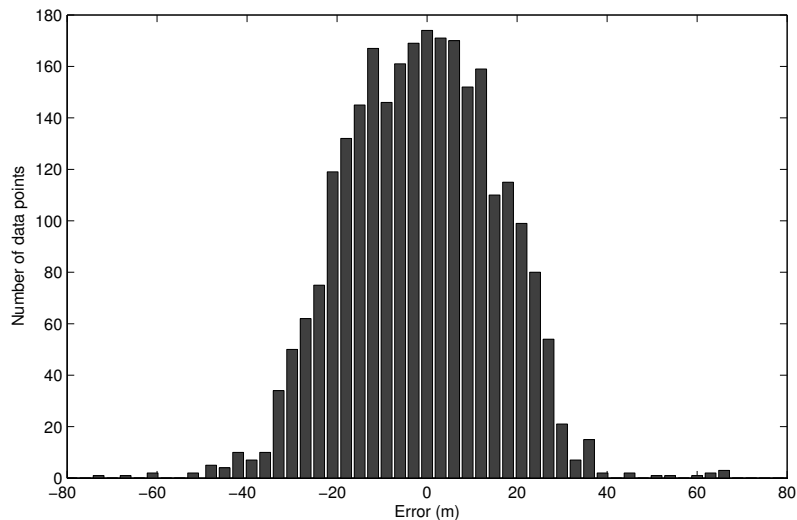


Fig. 18. The error distribution of the estimation results with average jet speed of 3 m/s and $k = 3$.

The effect of the variation in the average jet speed parameter of the meandering mobility model is also tested for the energy consumption. Fig. 15 shows the average energy consumption with 95% confidence interval for different values of average jet speed. When these results are combined with the results in Fig. 15, we observe that the energy consumption increases with the increasing values of both k and jet speed, and the selection of k value is more influential in terms of energy when utilizing the localization approach.

V. CONCLUSION

In this paper, a novel localization algorithm for wireless networks with mobile sensor nodes and stationary actors is proposed. The goal is to improve the on-site monitoring of Amazon river with a

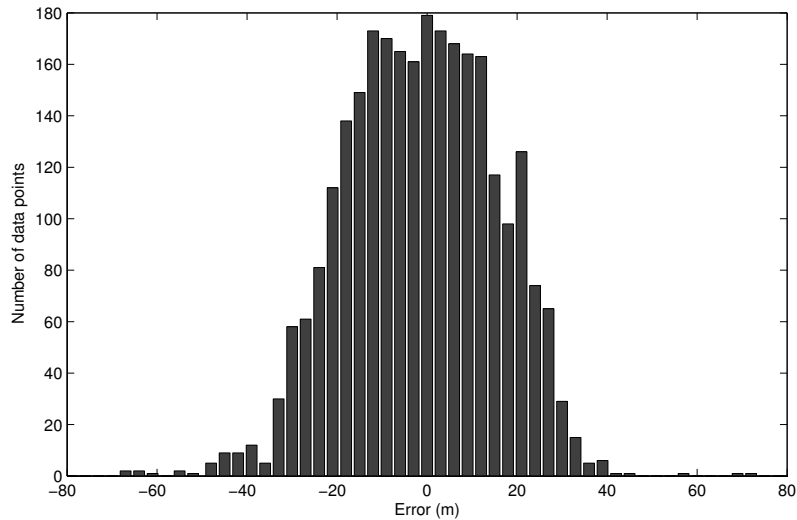


Fig. 19. The error distribution of the estimation results with average jet speed of 5 m/s and $k = 3$.

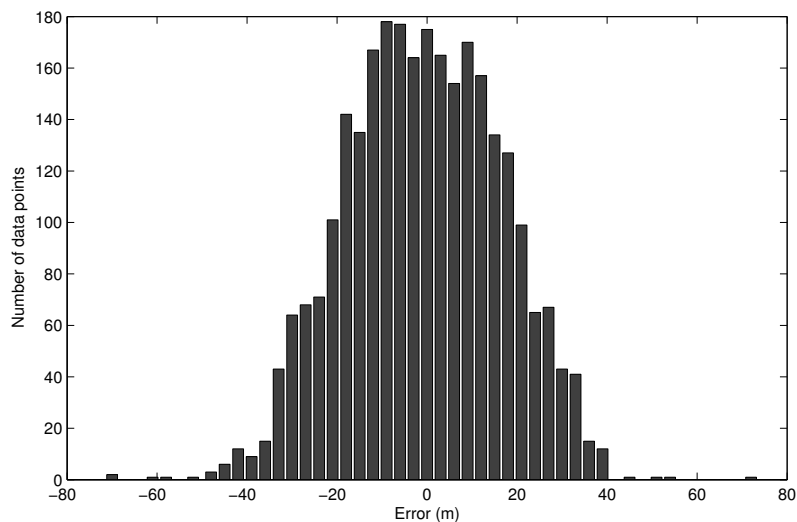


Fig. 20. The error distribution of the estimation results with average jet speed of 7 m/s and $k = 3$.

lightweight localization extension. The particular scenario has its own challenges, which require high adaptability to failures and high mobility of sensor nodes. The proposed localization algorithm overcomes these challenges by a locality preserving approach complemented with an idea that benefits from the motion pattern of the sensors. The algorithm aims to retrieve location information at the actor nodes rather than the sensors and it adopts 1-hop localization approach in order to address the limited lifetime of the WSN. The accuracy of the proposed algorithm can be further improved with RSS or other measurement techniques at the expense of increased energy consumption. The selection of a realistic mobility model is critical for performance evaluation of a localization algorithm. As another contribution of the paper, a subsurface current mobility model is adopted and tailored according to the requirements of

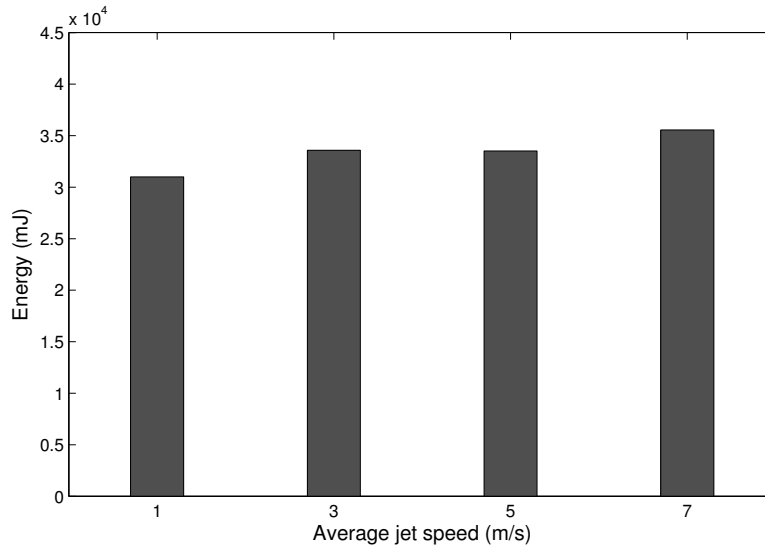


Fig. 21. Energy consumption for meandering mobility with different average jet speed values.

the scenario. Through extensive simulations, we have shown that the localization estimation can be realized using local multi-hop information. In overall, as the multi-hop chains are allowed to become longer, more positions can be estimated with the cost of lower accuracy. The selection of the maximum hop number is therefore an issue depending on the requirements of network. As future work, we are planning to integrate an actor positioning strategy with our approach since the actor positions and the communication in the network among actors affect the performance of localization. We intend to improve the routing and energy consumption by using the localization information for data aggregation and dissemination.

ACKNOWLEDGEMENT

The authors would like to thank OPNET Technologies Inc. for supporting this research by providing OPNET Modeler software under OPNET University Program.

REFERENCES

- [1] I. F. Akyildiz and I. H. Kasimoglu, "Wireless Sensor and Actor Networks: Research Challenges," *Ad Hoc Networks*, vol. 2, no. 4, pp. 351–367, October 2004.
- [2] J. Yick, B. Mukherjee, and D. Ghosal, "Wireless sensor network survey," *Computer Networks*, vol. 52, no. 12, pp. 2292–2330, 2008.
- [3] Y. Zheng and Y. Liu, "Understanding node localizability of wireless ad hoc and sensor networks," *IEEE Transactions on Mobile Computing*, vol. 11, no. 8, pp. 1249–1260, August 2012.
- [4] M. İ. Akbaş and M. R. Brust and D. Turgut, "Local Positioning for Environmental Monitoring in Wireless Sensor and Actor Networks," in *Proceedings of the IEEE Conference on Local Computer Networks (LCN)*, October 2010, pp. 806–813.

- [5] A. Caruso, F. Paparella, L. Vieira, M. Erol, and M. Gerla, "The Meandering Current Mobility Model and its Impact on Underwater Mobile Sensor Networks," in *Proceedings of the IEEE International Conference on Computer Communications (INFOCOM)*, April 2008, pp. 13–19.
- [6] J. M. A. Peixoto, B. W. Nelson, and F. Wittmann, "Spatial and temporal dynamics of river channel migration and vegetation in central Amazonian white-water floodplains by remote-sensing techniques," *Remote Sensing of Environment*, vol. 113, no. 10, pp. 2258 – 2266, 2009.
- [7] G. Mao, B. Fidan, and B. D. Anderson, "Wireless sensor network localization techniques," *Computer Networks*, vol. 51, no. 10, pp. 2529–2553, 2007.
- [8] W. Hu, N. Bulusu, and S. Jha, "A communication paradigm for hybrid sensor/actuator networks," in *Proceedings of the IEEE International Symposium on Personal, Indoor and Mobile Radio Communications (PIMRC)*, September 2004, pp. 201–205.
- [9] B. Turgut and R. P. Martin, "Using a-priori information to improve the accuracy of indoor dynamic localization," in *Proceedings of ACM International Conference on Modeling, Analysis, and Simulation of Wireless and Mobile Systems (MSWiM)*, October 2009, pp. 394–404.
- [10] B. D. Anderson, P. N. Belhumeur, T. Eren, D. K. Goldenberg, A. S. Morse, W. Whiteley, and Y. R. Yang, "Graphical properties of easily localizable sensor networks," *Wireless Networks*, vol. 15, no. 2, pp. 177–191, 2009.
- [11] J. Jeong, S. Guo, T. He, and D.-C. Du, "Autonomous Passive Localization Algorithm for Road Sensor Networks," *IEEE Transactions on Computers*, vol. 60, no. 11, pp. 1622–1637, 2011.
- [12] H. Shi, X. Li, Y. Shang, and D. Ma, "Error analysis of quantised RSSI based sensor network localisation," *International Journal of Wireless and Mobile Computing*, vol. 4, no. 1, pp. 31–40, 2010.
- [13] J. Paek, K.-H. Kim, J. P. Singh, and R. Govindan, "Energy-efficient positioning for smartphones using Cell-ID sequence matching," in *Proceedings of the International Conference on Mobile Systems, Applications, and Services (MobiSys)*, June 2011, pp. 293–306.
- [14] D. Niculescu and B. Nath, "DV based positioning in ad hoc networks," *Journal of Telecommunication Systems*, vol. 22, no. 4, pp. 267–280, 2003.
- [15] Y. Wang, S. Lederer, and J. Gao, "Connectivity-Based Sensor Network Localization with Incremental Delaunay Refinement Method," in *Proceedings of the IEEE International Conference on Computer Communications (INFOCOM)*, April 2009, pp. 2401–2409.
- [16] B. Turgut and R. P. Martin, "Restarting particle filters: an approach to improve the performance of dynamic indoor localization," in *Proceedings of the IEEE Global Communications Conference (GLOBECOM)*, November 2009, pp. 1–6.
- [17] B. Turgut and R. P. Martin, "A multi-hypothesis particle filter for indoor dynamic localization," in *Proceedings of the IEEE Conference on Local Computer Networks (LCN)*, October 2009, pp. 742–749.
- [18] B.-H. Liu, M.-L. Chen, and M.-J. Tsai, "Message-Efficient Location Prediction for Mobile Objects in Wireless Sensor Networks Using a Maximum Likelihood Technique," *IEEE Transactions on Computers*, vol. 60, no. 6, pp. 865–878, 2011.
- [19] H. Oliveira, A. Boukerche, E. Nakamura, and A. Loureiro, "An Efficient Directed Localization Recursion Protocol for Wireless Sensor Networks," *IEEE Transactions on Computers*, vol. 58, no. 5, pp. 677–691, 2009.
- [20] H. Xu, W. Liu, and B. Wang, "Subarea localization performance of the divide-and-cover node deployment in a long bounded belt scenario," *IEEE Transactions on Computers*, vol. PrePrints, no. 99, 2013.
- [21] J. Maneesilp, C. Wang, H. Wu, and N.-F. Tzeng, "RFID support for accurate 3D localization," *IEEE Transactions on Computers*, vol. 62, no. 7, pp. 1447–1459, 2013.
- [22] J. Chen, C. Wang, Y. Sun, and X. S. Shen, "Semi-supervised Laplacian regularized least squares algorithm for localization in wireless sensor networks," *Computer Networks*, vol. 55, no. 10, pp. 2481–2491, 2011.

- [23] B. Krishnamachari and S. Iyengar, "Distributed bayesian algorithms for fault-tolerant event region detection in wireless sensor networks," *IEEE Transactions on Computers*, vol. 53, no. 3, pp. 241–250, 2004.
- [24] I. A. Getting, "The global positioning system," *IEEE Spectrum*, vol. 30, no. 12, pp. 36–47, December 1993.
- [25] L. Yang and K. Ho, "An approximately efficient TDOA localization algorithm in closed-form for locating multiple disjoint sources with erroneous sensor positions," *IEEE Transactions on Signal Processing*, vol. 57, no. 12, pp. 4598–4615, 2009.
- [26] T. Eren, "Cooperative localization in wireless ad hoc and sensor networks using hybrid distance and bearing (angle of arrival) measurements," *EURASIP Journal on Wireless Communications and Networking*, vol. 2011, no. 1, pp. 1–18, 2011.
- [27] B. Turgut and R. P. Martin, "Localization for indoor wireless networks using minimum intersection areas of iso-RSS lines," in *Proceedings of the IEEE Local Computer Networks (LCN)*, October 2007, pp. 962–972.
- [28] H. Ahn, Y.-H. Lee, H.-J. Cho, S.-B. Rhee, and J.-H. Lee, "A RSSI-Based Approach for Localization of Wireless Sensor Network in Indoor," in *Proceedings of the International Conference on IT Convergence and Security (ICITCS)*, December 2012, pp. 123–127.
- [29] S. Rallapalli, L. Qiu, Y. Zhang, and Y.-C. Chen, "Exploiting temporal stability and low-rank structure for localization in mobile networks," in *Proceedings of the International Conference on Mobile Computing and Networking (MobiCom)*, September 2010, pp. 161–172.
- [30] H. Wang, S. Sen, A. Elgohary, M. Elgohary, M. Youssef, and R. R. Choudhury, "No need to war-drive: unsupervised indoor localization," in *Proceedings of the International Conference on Mobile Systems, Applications, and Services (MobiSys)*, 2012, pp. 197–210.
- [31] M. Michaelides and C. Panayiotou, "SNAP: Fault Tolerant Event Location Estimation in Sensor Networks Using Binary Data," *IEEE Transactions on Computers*, vol. 58, no. 9, pp. 1185–1197, 2009.
- [32] R. Nagpal, H. Shrobe, and J. Bachrach, "Organizing a global coordinate system from local information on an ad hoc sensor network," in *Proceedings of the International Conference on Information Processing in Sensor Networks (IPSN)*, April 2003, pp. 333–348.
- [33] J.-P. Sheu, W.-K. Hu and J.-C. Lin, "Distributed Localization Scheme for Mobile Sensor Networks," *IEEE Transactions on Mobile Computing*, vol. 9, no. 4, pp. 516–526, April 2010.
- [34] M. Rahman and L. Kleeman, "Paired Measurement Localization: A Robust Approach for Wireless Localization," *IEEE Transactions on Mobile Computing*, vol. 8, no. 8, pp. 1087–1102, August 2009.
- [35] B. Xiao, L. Chen, Q. Xiao, and M. Li, "Reliable Anchor-Based Sensor Localization in Irregular Areas," *IEEE Transactions on Mobile Computing*, vol. 9, pp. 60–72, 2010.
- [36] J. Yi, S. Yang, and H. Cha, "Multi-hop-based monte carlo localization for mobile sensor networks," in *Proceedings of IEEE Communications Society Conference on Sensor, Mesh and Ad Hoc Communications and Networks (SECON)*, June 2007, pp. 162–171.
- [37] G. Wu, S. Wang, B. Wang, Y. Dong, and S. Yan, "A novel range-free localization based on regulated neighborhood distance for wireless ad hoc and sensor networks," *Computer Networks*, vol. 56, no. 16, pp. 3581–3593, 2012.
- [38] M. I. Akbaş, M. R. Brust, and D. Turgut, "SOFROP: Self-Organizing and Fair Routing Protocol for Wireless Networks with Mobile Sensors and Stationary Actors," *Elsevier's Computer Communications Journal (Special Issue on Specialized Routing and Node Placement Protocols for Emerging Wireless Ad Hoc Networks)*, vol. 34, no. 18, pp. 2135–2146, December 2011.
- [39] M. Chatterjee, S. Das, and D. Turgut, "WCA: A weighted clustering algorithm for mobile ad hoc networks," *Journal of Cluster Computing (Special Issue on Mobile Ad hoc Networks)*, vol. 5, no. 2, pp. 193–204, April 2002.
- [40] D. Turgut, S. Das, R. Elmasri, and B. Turgut, "Optimizing clustering algorithm in mobile ad hoc networks using genetic algorithmic approach," in *Proceedings of IEEE Global Telecommunications Conference (GLOBECOM)*, November 2002, pp. 62–66.
- [41] D. Turgut, B. Turgut, R. Elmasri, and T. V. Le, "Optimizing clustering algorithm in mobile ad hoc networks using simulated annealing," in *Proceedings of Wireless Communications and Networking Conference (WCNC)*, March 2003, pp. 1492–1497.

- [42] N. Aydin, F. Nait-Abdesselam, V. Pryyma, and D. Turgut, "Overlapping clusters algorithm in ad hoc networks," in *Proceedings of the IEEE Global Telecommunications Conference (GLOBECOM)*, December 2010, pp. 1–5.
- [43] O. Younis and S. Fahmy, "Distributed Clustering in Ad-hoc Sensor Networks: A Hybrid, Energy-Efficient Approach," in *Proceedings of the IEEE International Conference on Communications (INFOCOM)*, March 2004, pp. 629–640.
- [44] M. Erol, L. Vieira, A. Caruso, F. Paparella, M. Gerla, and S. Oktug, "Multi stage underwater sensor localization using mobile beacons," in *Proceedings of the Workshop on Under Water Sensors and Systems (in conjunction with SENSORCOMM)*, August 2008, pp. 25–31.
- [45] A. V. M. Cencini, G. Lacorata and E. Zambianchi, "Mixing in a Meandering Jet: A Markovian Approximation," *Journal of Physical Oceanography*, vol. 29, no. 10, pp. 2578–2594, 1999.
- [46] A. S. Bower, "A Simple Kinematic Mechanism for Mixing Fluid Parcels Across a Meandering Jet," *Journal of Physical Oceanography*, vol. 21, no. 1, pp. 173–180, 1991.
- [47] R. M. Samelson, "Fluid exchange across a meandering jet," *Journal of Physical Oceanography*, vol. 22, no. 4, pp. 431–444, 1992.
- [48] "OPNET Modeler," <http://www.opnet.com>.
- [49] F. Regan, A. Lawlor, B. Flynn, J. Torres, R. Martinez-Catala, C. O'Mathuna, and J. Wallace, "A demonstration of wireless sensing for long term monitoring of water quality," in *Proceedings of the IEEE Conference on Local Computer Networks (LCN)*, October 2009, pp. 819–825.